Inflammation
https://doi.org/10.1007/s10753-025-02322-4

RESEARCH

Evaluation of Cardiac IL-11 and IL-11Rα Expression During *T. cruzi* Infection

Yarlla Loyane Lira Braga[1] · José Rodrigues do Carmo Neto[1] · Pablo Igor Ribeiro Franco[1] · Jordana Fernandes de Oliveira[1] · Rafael Obata Trevisan[3] · Fernanda Bernadelli de Vito[4] · Flávia Aparecida de Oliveira[1] · Mara Rúbia Nunes Celes[1] · Marcos Vinícius da Silva[2] · Juliana Reis Machado[1,3]

Received: 22 January 2025 / Revised: 7 May 2025 / Accepted: 23 May 2025

Abstract

Chagas disease (CD), caused by *Trypanosoma cruzi*, leads to cardiomyopathy in approximately 20–30% of infected individuals. Interleukin-11 (IL-11) has been implicated in cardiac fibrosis, although its immunological role in this context remains unclear. This study investigated the temporal dynamics of IL-11 and its receptor, IL-11Rα, expression in the hearts of C57BL/6 mice infected with 1,000 trypomastigote forms of the Y or Colombian strains of *T. cruzi*. Mice were euthanized at 5, 15, 30, 60, and 120 days post-infection (dpi). Survival, parasitemia, and body and heart weights were monitored. Cardiac tissue was analyzed for parasite nests, myocarditis, collagen deposition, and expression of the IL-11 receptor alpha (IL-11Rα). Cytokine profiles were evaluated by ELISA and Cytometric Bead Array. Histopathological analysis revealed more intense myocarditis, parasite load, and collagen deposition in mice infected with the Colombian strain. Both strains induced IFN-γ, TNF-α, and IL-6 in cardiac tissue; however, IL-10, IL-4, and IL-17 were detected only in the Y strain, indicating a more balanced immune response. Despite the absence of significant IL-11 upregulation in either infection, IL-11Rα expression was progressively increased over time and positively correlated with collagen deposition. These findings suggest that IL-11Rα may play a role in cardiac remodeling and fibrosis independently of IL-11 upregulation. The results reinforce the importance of *T. cruzi* strain variability in disease outcome and highlight the IL-11/IL-11Rα axis as a potential target for further investigation in Chagas cardiomyopathy.

Graphical Abstract

The kinetics of IL-11 and IL-11Rα expression in the heart during experimental *Trypanosoma cruzi* infection reveal striking differences between the Y and Colombian strains over time (5, 15, 30, 60, and 120 days post-infection). The shaded areas in green and orange represent IL-11Rα expression and IL-11 production, respectively. In the Y strain, IL-11 production is

✉ Juliana Reis Machado
juliana.patologiageral@gmail.com

Yarlla Loyane Lira Braga
yarlla_lira@hotmail.com

José Rodrigues do Carmo Neto
rodriguesnneto@gmail.com

Pablo Igor Ribeiro Franco
pablo_igor@hotmail.com

Jordana Fernandes de Oliveira
jordana.fer@hotmail.com

Rafael Obata Trevisan
rafaelotrevisan@gmail.com

Fernanda Bernadelli de Vito
fernanda.vito@uftm.edu.br

Flávia Aparecida de Oliveira
flavia@ufg.br

Mara Rúbia Nunes Celes
mrubia_celes@ufg.br

Marcos Vinícius da Silva
marcos.silva@uftm.edu.br

[1] Department of Bioscience and Technology, Institute of Tropical Pathology and Public Health, Federal University of Goiás, Goiânia, GO 74605-450, Brazil

[2] Department of Microbiology, Immunology and Parasitology, Institute of Biological and Natural Sciences, Federal University of Triângulo Mineiro, Uberaba, Minas Gerais 38025-180, Brazil

[3] General Pathology, Federal University of Triângulo Mineiro, Uberaba, Minas Gerais, Brazil

[4] Hematological Research Laboratory, Federal University of Triângulo Mineiro, Uberaba, MG 38025-180, Brazil

Published online: 12 September 2025

detectable throughout the infection, peaking around 30 days. In contrast, the Colombian strain exhibits lower IL-11 expression. IL-11Rα expression is upregulated in both strains: starting at 15 dpi in the Y strain and at 60 dpi in the Colombian strain, remaining elevated until 120 dpi. The colored lines indicate the kinetics of other parameters: Pro-inflammatory cytokines (TNF-α, IFN-γ, IL-6): red; Regulatory/Th2/Th17 cytokines (IL-10, IL-4, IL-17): green; Cardiac parasitism (*T. cruzi* nests): purple; Inflammatory infiltrate: black; Collagen deposition: brown. The distinct peaks observed between groups reflect the specific immunopathological characteristics of each strain in terms of inflammation, immune response, and cardiac damage. This graphic scheme provides an integrated summary of the dynamics between the analyzed parameters throughout the course of infection.

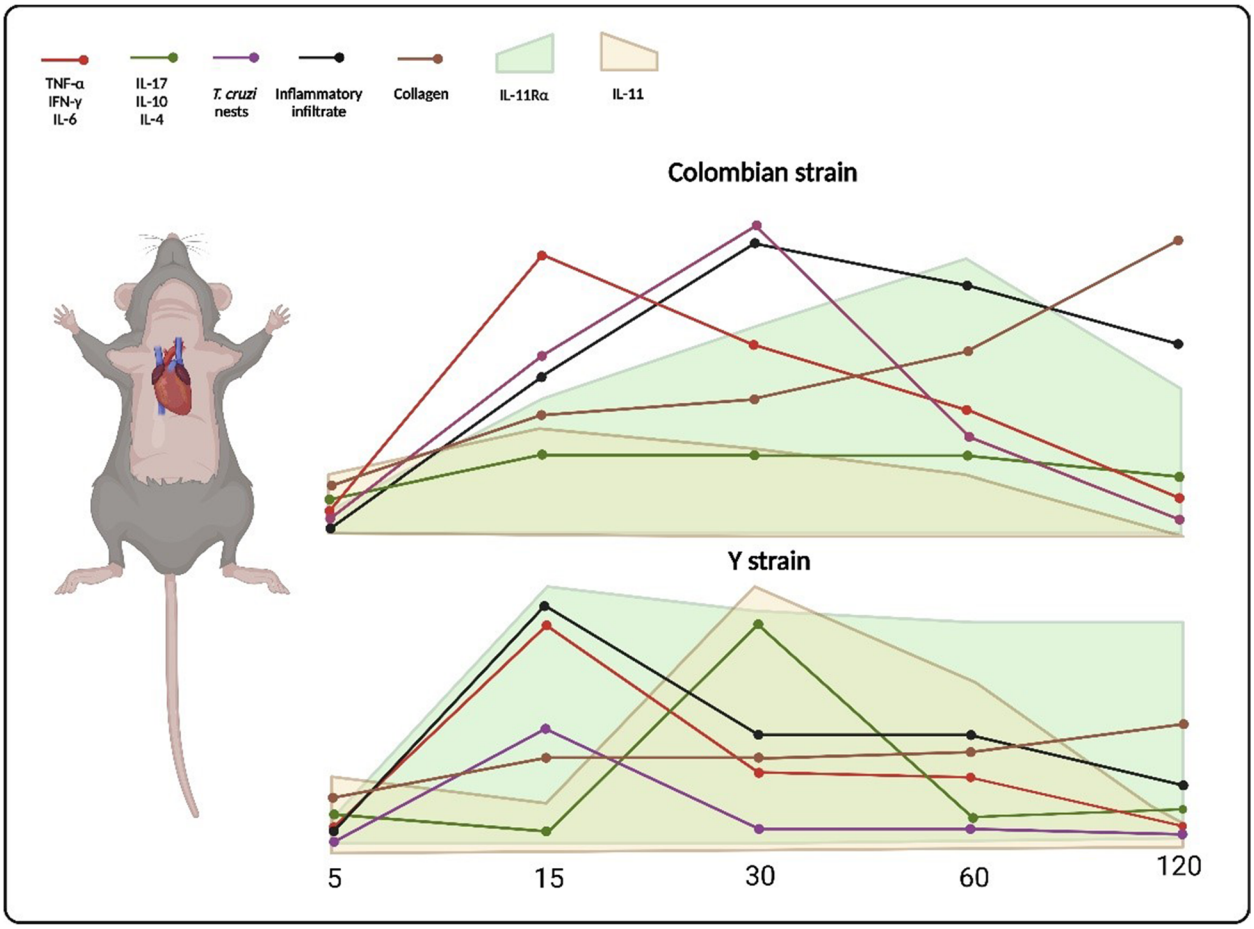

Keywords Interleukin (IL)-11 · *Trypanosoma cruzi* · Cellular immune response · Cardiomyopathy · DTUs · Chagas disease

Background

Chagas disease (CD) is a parasitic infection caused by *Trypanosoma cruzi*, with cardiomyopathy being one of its most prominent pathological manifestations, affecting 20–30% of infected individuals [1]. In endemic areas such as Central and South America, CD is a leading cause of heart disease and cardiovascular-related deaths [2]. The severity of chronic Chagas cardiomyopathy (CCC) is strongly associated with the magnitude of cardiac injury sustained during the acute phase of infection [3]. This damage evolves over time, culminating in persistent cardiac inflammation and remodeling.

Cardiac alterations during the chronic phase are primarily characterized by a mononuclear cell infiltrate, predominantly consisting of macrophages, CD4 + and CD8 + T cells, myocardial fiber destruction in the inflammatory focus and scarce parasites in the lesion [4, 5]. Despite extensive research, the pathogenesis of CCC remains incompletely understood. The balance between the inflammatory immune response and parasite control in the acute phase, as well as the genetic and pathogenic diversity

among *T. cruzi* strains, are considered pivotal determinants of disease progression and clinical outcome [2, 5, 6].

Among the pathological hallmarks of CCC, diffuse myocardial fibrosis plays a central role and is closely associated with cardiac dysfunction in human patients [7–9]. Recent studies have identified interleukin-11 (IL-11) as a key pro-fibrotic cytokine in the heart, capable of promoting fibroblast-to-myofibroblast transition and acting downstream of TGF-β to enhance extracellular matrix production [10–13]. Importantly, therapeutic inhibition of IL-11 has shown promise in reversing fibrosis in various experimental models, positioning this cytokine as a potential therapeutic target [13–17].

In addition to its pro-fibrotic role, IL-11 exhibits diverse immunological functions. It can modulate Th2-type immune responses, stimulate Th17 cell activity, and trigger pro-inflammatory signaling pathways [18–22]. IL-11 has also been implicated in the progression of chronic inflammatory diseases and in host responses to viral and bacterial infections [23–25]. During *T. cruzi* infection, in vitro studies have demonstrated that IL-11 expression may vary depending on the strain involved, suggesting a strain-dependent immunomodulatory function [26, 27].

Given this background, the present study aims to investigate the temporal dynamics of cardiac IL-11 and IL-11Rα expression in a murine model of Chagas disease, using two *T. cruzi* strains from distinct Discrete Typing Units (DTUs). By correlating these findings with inflammatory responses and cardiac remodeling, we seek to clarify the potential role of the IL-11/IL-11Rα axis in the pathogenesis of CCC and its relationship with parasite genetic variability.

Methodology

Study Aim, Design, and Setting

The aim of this study was to evaluate the cytokines production and cardiac alterations in mice infected with different strains of *Trypanosoma cruzi* at 5, 15, 30, 60 and 120 days of infection. This is an experimental study conducted under controlled laboratory conditions, where the animals were housed under regulated light cycles and temperature, with free access to water and food.

Animal Model and Experimental Design

Male C57Bl/6 mice were 8–10 weeks of age (22–27 g), both infected and non-infected, were used in this study. C57Bl/6 mice are frequently used as a model for experimental CD and are described as an easily inducible chronic model with a predominantly Th1 response profile [28, 29]. Male mice were specifically selected due to their consistent and reproducible immune and pathological responses, especially regarding cardiac tissue involvement [30, 31]. The infection was carried out using blood trypomastigotes derived from BALB/c mice. Parasite count was determined by examining 50 fields in a 5 µL blood sample placed between a slide and coverslip [32]. Infected animals were inoculated subcutaneously in the abdominal region with 1,000 trypomastigote forms of either the Colombian or Y strain. The study comprised eleven groups: one uninfected control group and ten infected groups. Infected groups were further divided based on the strain and days post-infection (dpi) (Table 1). Mice were euthanized at 5, 15, 30, 60, and 120 dpi to capture different phases of the disease. Necropsy was performed through a dorsolateral incision, with the heart collected for in situ study and histopathological analyses.

Evaluation of Parasite Load, Survival, and Body Weight

Parasitemia in infected mice was assessed using the Brener method (1962). Blood was obtained via a small puncture (< 1 mm) at the tip of the tail, with 5 µL of blood placed between a slide and coverslip. The number of parasites was determined across 50 random fields at 400 × magnification using a light microscope. Results were subjected to correction factor calculations based on the coverslip area and the field observed. Mice were also weighed on the day of infection and at euthanasia.

Cardiac Tissue Homogenization

After heart extraction, the organ was transversally divided into two portions. The apex fragments were stored at −80 °C in PBS solution containing a Complete™ protease inhibitor. The fragments were then homogenized using a DREMEL®300

Table 1 Experimental groups

Group	Infected/Non-infected	Days post-infection	Number of animals
Control group	Non-infected	-	6
Y	Infected	5	6
Col	Infected	5	6
Y	Infected	15	6
Col	Infected	15	6
Y	Infected	30	6
Col	Infected	30	6
Y	Infected	60	6
Col	Infected	60	6
Y	Infected	120	6
Col	Infected	120	11

homogenizer (Marconi, Ribeirão Preto, Brazil). The homogenate was centrifuged, and the supernatant stored at −80 °C for subsequent cytokine and total protein quantification. Total proteins were quantified using NanoDrop™ 2000/2000c spectrophotometers (Thermo Scientific™).

Histopathological Evaluation

The other portion of the heart was processed for histopathological evaluations. Myocarditis assessment, amastigote nest quantification, and collagen deposition were restricted to the cardiac ventricles. HE-stained sections were used to quantify inflammatory cell infiltrates and tissue parasitism. Myocarditis and tissue parasitism were evaluated in serial sections, capturing 10 random fields per fragment. Analyses were performed using a digital camera attached to a microscope. For tissue parasitism, slides were photographed at 40 × magnification using a digital camera attached to a microscope (Leica QWin), with results expressed as parasites/field (adapted from Wesley et al., 2019 [30]). The following formula was applied to calculate the result:

$$\text{Parasite/field} = \frac{\text{Average number of amastigote nests in the three fragments}}{30}$$

For the inflammatory infiltrate, slides were photographed at 20 × magnification. Inflammation intensity was categorized as 0 (normal), 1 (mild), 2 (moderate), or 3 (severe). The average score for each case was classified as follows: 0–0.3 = normal; 0.4–1.0 = mild; 1.1–2 = moderate; 2.1–3 = severe [30]. Results were presented in score form using the following formula:

$$\text{Inflammatory infiltrate (score)} = \frac{\sum \textit{intensity of the inflammatory process in the 30 fields}}{30}$$

Collagen deposition was evaluated in Picro-Sirius stained sections counterstained with hematoxylin for one minute. Ten random fields from the left and right ventricles were captured and quantified at 20 × magnification using polarized light microscopy. Morphometry was performed using Axion Vision software (ZEISS), with results expressed as a percentage of collagen per animal [33].

IL-11Rα Expression by Western Blotting

Cardiac homogenates from control and infected groups (both *T. cruzi* strains) were analyzed for IL-11Rα expression via Western Blotting. Protein extracts were loaded onto 10% SDS-PAGE gels. A volume of 25 µL of each sample was loaded per lane. After electrophoresis, proteins were transferred to a PVDF membrane (Immobilon®-Psq, Millipore Corporation, Billerica, MA, USA), which was blocked with 5% BSA (Sigma-Aldrich) overnight at 4 °C. The membrane was then washed in PBS-T buffer and incubated overnight at 4 °C with the primary anti-IL-11Rα antibody (sc393057, Santa Cruz Biotechnology) diluted in 1% BSA PBS-T buffer. For loading control, the membrane was also incubated with an anti-GAPDH antibody (BA1050, Booster) at a 1:10.000 dilution under the same conditions. After washing, the membrane was incubated with an HRP-conjugated anti-rabbit secondary antibody for 45 min at room temperature. The membrane was developed using ECL solution (ECL Kit; GE Healthcare Bio-Sciences) as per the manufacturer's instructions and visualized using the ChemiDoc XRS system (BioRad). Band quantification was performed using ImageJ software, with results reported as optical density (OD) in arbitrary units (AU).

Immunohistochemistry for IL-11Rα

Immunohistochemistry for IL-11Rα (sc393057, Santa Cruz Biotechnology) was performed on heart sections from infected and control mice. The fragments were fixed in formaldehyde. Endogenous peroxidase activity was blocked by treating the slides with H2O2 in methanol, followed by washes and incubation in PBS containing 2% PBS-BSA. Sections were incubated with the primary antibody at a 1:70 dilution for 3 h at 37 °C. After washing in PBS, the sections were incubated for 2 h with the LSAB detection kit, followed by DAB staining for 5 min. The reaction was halted by rinsing the slides in running water. The sections were counterstained with hematoxylin and mounted for light microscopy analysis. This technique was used to demonstrate receptor presence in the tissue, with no statistical analysis performed.

Cytokine Measurement – CBA and ELISA

Levels of IFN-γ, TNF-α, IL-10, IL-6, IL-17, and IL-4 in cardiac homogenates were measured using the Cytometric Bead Array (CBA) technique (Mouse Th1/Th2/Th17 CBA Kit—BD™ Cytometric Bead Array (CBA), San Jose, CA, USA) according to the manufacturer's protocol. Beads bound to the cytokines were resuspended in 200 µL of washing buffer and transferred to cytometry tubes for acquisition, which was performed using a BD FACSCalibur flow cytometer (BD Biosciences, USA). Acquisition analysis was performed using FCAP Array™ software version 2.0 (BD Biosciences, USA), and cytokine concentrations were estimated via linear regression analysis using the fluorescence obtained from each cytokine's standard curve, expressed in pg/mL. For final results, each cytokine's value was normalized to total protein content in the cardiac tissue.

Cardiac homogenate IL-11 levels were quantified using a sandwich ELISA (R&D Systems), following the manufacturer's instructions. The reaction was halted with 0.4 M sulfuric acid (25 µL per well). Plates were read at 450 nm

in a microplate reader, and cytokine concentrations were determined by regression analysis, comparing the absorbance of the samples with standard curves.

Statistical Analysis

Data were tabulated using EXCEL 2016 for WINDOWS (MICROSOFT – USA) and analyzed using GRAPHPAD PRISM 7.0 software (GRAPHPAD SOFTWARE – USA). The Shapiro–Wilk test was used to assess the normality of quantitative data. For comparisons among two groups, one-way ANOVA was applied for normally distributed data, and the Kruskal–Wallis test for non-parametric data. Spearman's correlation was used for correlation analysis. Results were considered statistically significant when $p < 0.05$.

Results

Parasitemia, Amastigote Nests and Inflammatory Infiltrate Infected of Animals with Y and Colombian Strains at Different Phases of Infection of *T. cruzi*

During the infection with the Y and Colombian strains, distinct parasitemia profiles were observed between the groups. For the Y strain, parasitemia was detectable on day 5, peaking on day 15, and clearing by day 30 (Fig. 1A). For the Colombian strain, parasitemia became detectable on day 10, peaked on day 30, and cleared by day 70 post-infection (Fig. 1A).

Histological analysis showed amastigote nests in the heart tissue of infected mice. For the Colombian strain, nests were observed starting on day 15 and persisted until day 120, with the highest number observed on day 30 ($p < 0{,}0001$) (Fig. 1B and L). For the Y strain, nests were present only on day 15 ($p = 0{,}0183$) (Fig. 1B and M), indicating lower persistence of the infection.

The inflammatory infiltrate in the heart was significantly more intense in the infection with the Colombian strain, starting on day 15 and persisting until day 120 ($p < 0{,}0001$) (Fig. 1C, H, I, J, and K). For the Y strain, the inflammatory infiltrate was milder on day 15 ($p < 0{,}0001$) 30 and 60 days ($p = 0{,}0006$) (Fig. 1C, D, E, F, and H).

Body and Heart Weight

Regarding body weight, a significant reduction was observed in animals infected with the Colombian strain at 30 ($p < 0{,}0005$), 60 ($p < 0{,}0001$) and 120 ($p = 0{,}0207$) days post-infection, while for the Y strain, the reduction was observed with 30 ($p = < 0{,}0007$) days post-infection (Fig. 2A). The heart weight, normalized to body weight, was also significantly increased in the Colombian strain-infected animals at 30 ($p = 0{,}0240$) and 60 days ($p = 0{,}0259$), whereas for the Y strain, the increase was observed only at 15 days post-infection ($p = 0{,}0077$) (Fig. 2B).

Collagen Deposition Correlates Positively with IL-11Rα Expression in Both *T. cruzi* Strains

The collagen analysis in heart tissue revealed that infection with the Colombian strain induced a significant increase in collagen deposition at 60 days ($p = 0.0053$) and 120 days post-infection ($p < 0.0001$), as observed in the photomicrographs of infected hearts (Fig. 3A, F, and G). In animals infected with the Y strain, significant changes in collagen deposition were observed at 15 ($p = 0.0123$), 30 ($p = 0.0116$), 60 ($p = 0.0135$), and 120 days post-infection ($p < 0.0001$) (Fig. 3A, D, and E). These findings, together with the observed IL-11Rα expression patterns, revealed a positive correlation between IL-11Rα levels and collagen deposition in both the Y ($p = 0.0049$) and Colombian ($p < 0.0001$) strains, suggesting a potential role for this receptor in strain-dependent fibrotic responses during *T. cruzi* infection (Fig. 3B and C).

IL-11 Expression is not Significantly Altered During *T. cruzi* Infection, while IL-11Rα is Upregulated

IL-11 was produced in the heart during infection, but did not show a significant increase in either strain (Fig. 4A). The expression of IL-11Rα showed a significant increase in both strains, particularly on days 60 ($p < 0{,}0005$) and 120 ($p = 0{,}0174$) for the Colombian strain and on days 15, 30, 60, and 120 for the Y strain ($p < 0{,}0001$) (Fig. 4B and C). However, there was a positive correlation between IL-11Rα expression and collagen deposition in both strains in the heart ($p = 0{,}0049$ and $p < 0{,}0001$). Immunohistochemistry revealed IL-11Rα staining in various cardiac cells of the infected groups (Fig. 4D to M).

Cytokine Profile Induced by Infection

Cytokine measurements in the heart revealed that infection with the Colombian strain induced a pro-inflammatory response, with significant increases in IFN-γ, TNF-α, and IL-6 at several time points post-infection, particularly at days 15, 30, and 60 (IFN-γ $p < 0{,}0001$, $p = 0{,}0006$ and $p = 0{,}0010$) (TNF-α $p = 0{,}0008$, $p = 0{,}0002$ and $p = 0{,}0068$) (IL-6 $p < 0{,}0001$, $p < 0{,}0001$ and $p = 0{,}0040$) (Fig. 5A-C). In contrast, the Y strain induced a more balanced response, with an increase in Th1 and IL-6 cytokines peaking on day 15 of infection (IFN-γ $p < 0{,}0001$, TNF-α $p = 0{,}0034$ and IL-6 $p = 0{,}0005$) and

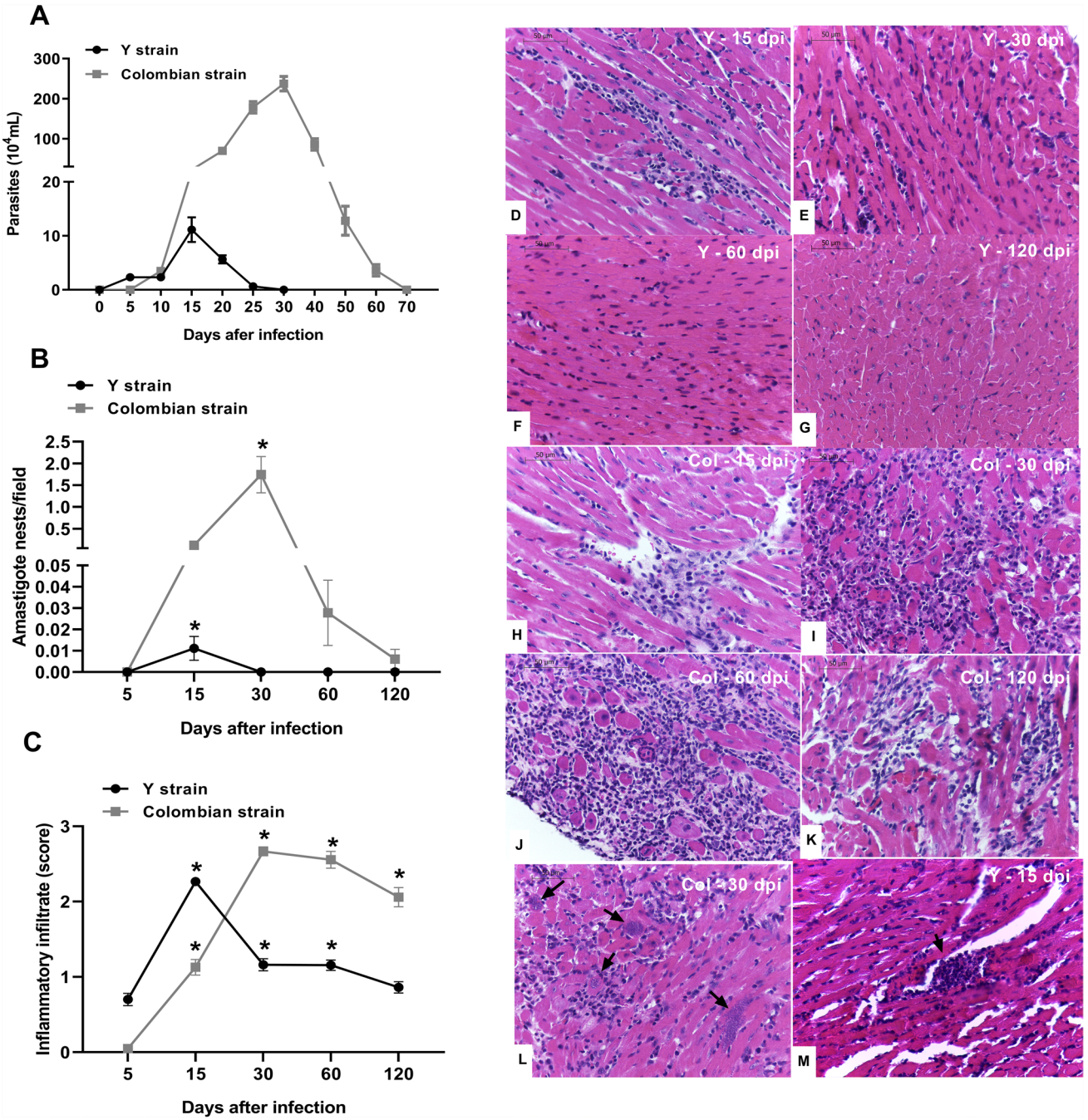

Fig. 1 **A** Parasitemia levels of animals infected with 1000 forms of the Y and Colombian strains via subcutaneous route. The data are representative, and no statistical comparisons between groups were performed. **B** *T. cruzi* nests and **C** Inflammatory cell infiltrate in the hearts of mice infected with the Y and Colombian strains at strains at 5 ($n = 6$), 15 ($n = 6$), 30 ($n = 6$), 60 ($n = 6$), and 120 dpi ($n = 6$ for Y and $n = 11$ for Colombian). **D**, **E**, **F** and **G** Photomicrographs (40x) of hearts from mice infected with 1000 forms of the *T. cruzi* Y strain at 15, 30, 60 and 120 dpi, respectively. **H**. **I**, **J** and **K** Photomicrographs of hearts from mice infected with 1000 forms of the *T. cruzi* Colombian strain at 15, 30, 60, and 120 dpi, respectively. Photomicrographs of heart tissue from mice infected with the Colombian strain at 30 days **L** and the Y strain at 15 days M. The black arrow indicates amastigote nests in the heart. *Statistically significant differences were observed between 5 dpi and 15, 30, 60, and 120 dpi ($p < 0.05$)

30 days only for TNF-α ($p = 0{,}0129$), followed by an increase in Th2 cytokines (IL-10 $p = 0{,}0138$ and IL-4 $p = 0{,}0003$), as well as IL-17 ($p = 0{,}0113$) (Fig. 5D-F). This balanced immune response likely contributes to the reduced severity of infection with the Y strain compared to the Colombian strain.

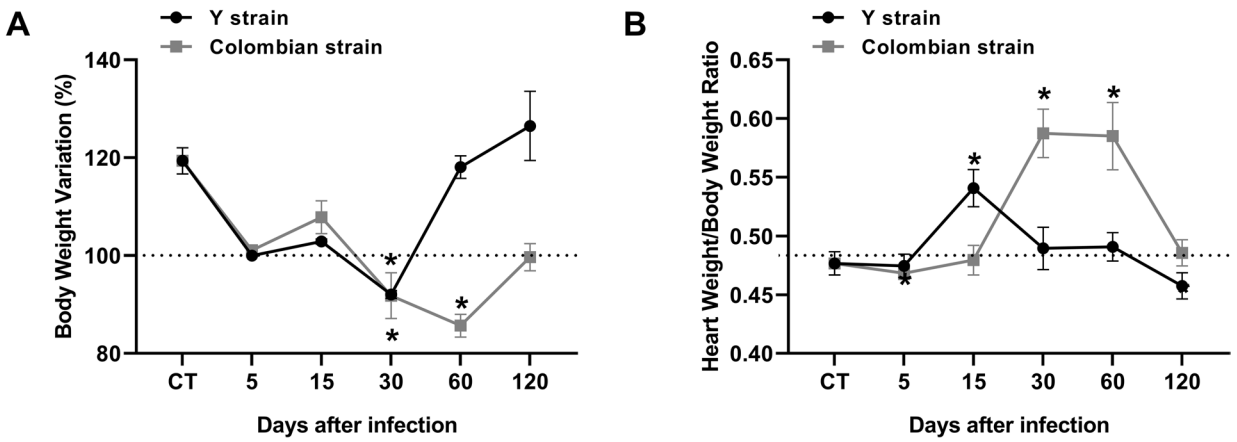

Fig. 2 Body and heart weight (%) of control and infected animals with 1000 forms of the Y and Colombian strains via subcutaneous injection on different days of infection at 5 ($n = 6$), 15 ($n = 6$), 30 ($n = 6$), 60 ($n = 6$), and 120 dpi ($n = 6$ for Y and $n = 11$ for Colombian). **A** Variation in body weight of animals infected with the Y and Colombian strains. **B** Heart weight to body weight ratio of mice infected with the Colombian and Y strains at 5, 15, 30, 60, and 120 days. *Statistically significant differences between infected and control (CT) groups, considering $p < 0.05$

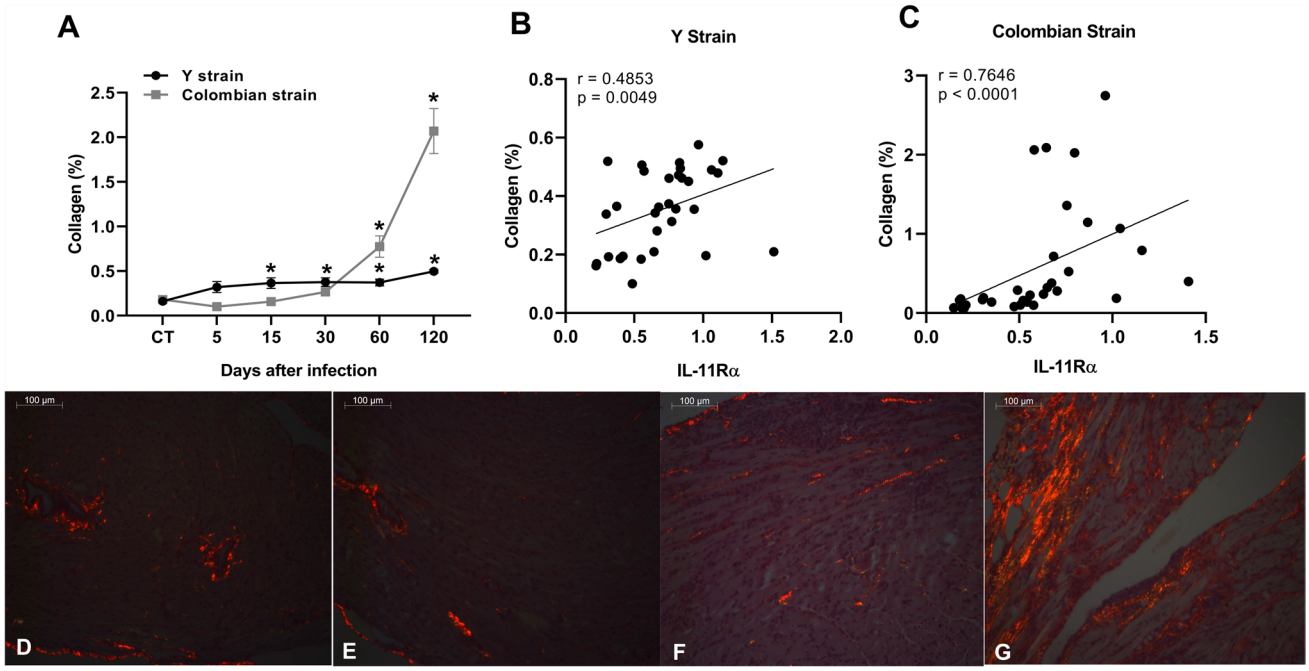

Fig. 3 Collagen analysis was performed by capturing 10 random fields in the ventricles using a 20 × objective, and quantification was done using the ACTION program. **A** Percentage (%) of collagen deposition in the hearts of mice infected with 1000 forms of the Colombian and Y strains at 5, 15, 30, 60, and 120 dpi. **B** and **C** Correlation was assessed between IL-11Rα expression and collagen deposition in cardiac tissue from animals infected with the Y and Colombian strains. **D** and **E** Photomicrographs of hearts from mice infected with the Y strain at 30 and 120 days post-infection, respectively. **F** and **G** Photomicrographs of hearts from mice infected with the Colombian strain at 30- and 120-days post-infection, respectively. *Statistically significant differences between infected and control (CT) groups, considering $p < 0.05$

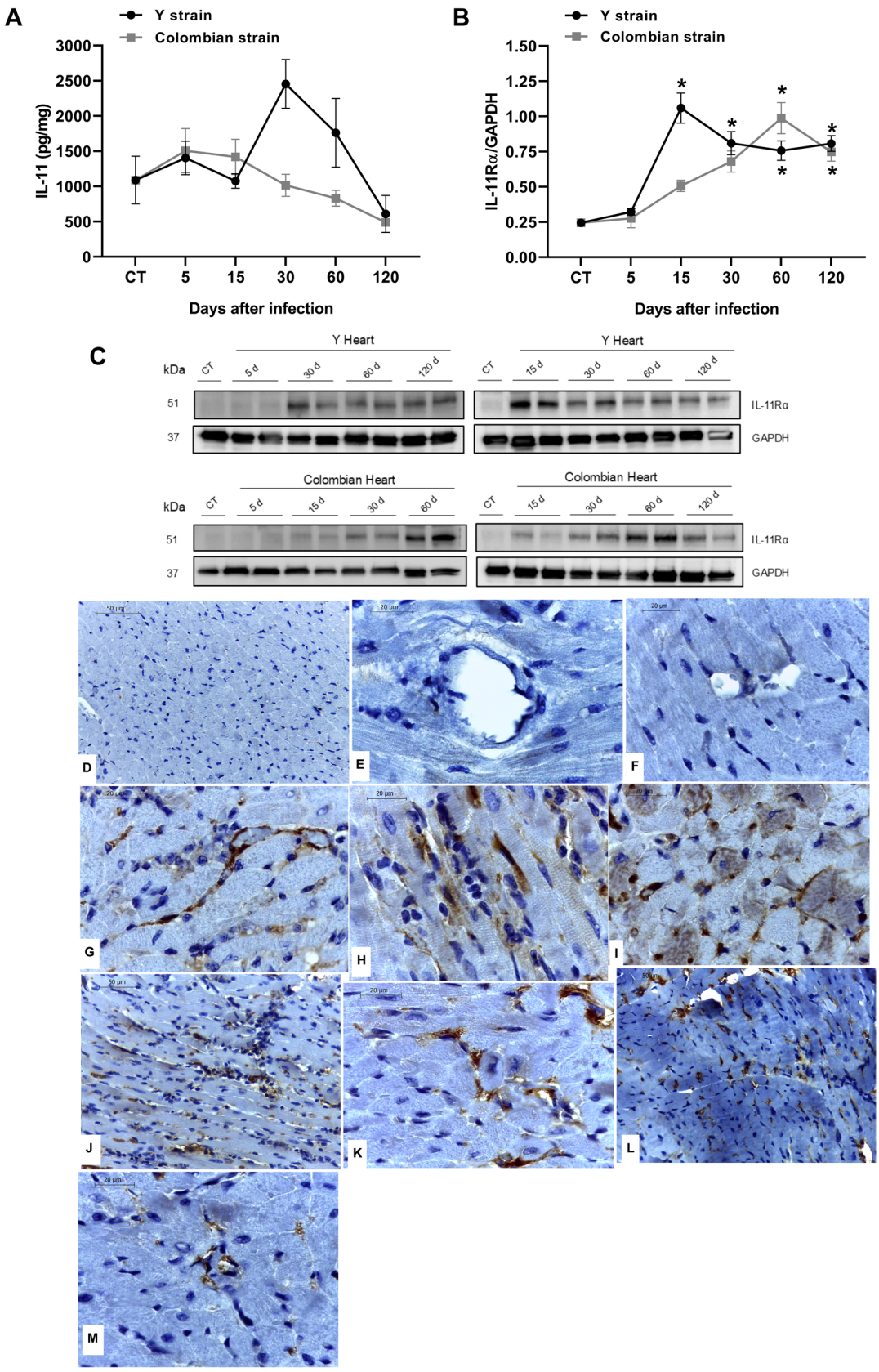
A
Y strain
Colombian strain
IL-11 (pg/mg)
3000
2500
2000
1500
1000
500
0
CT
5
15
30
60
120
Days after infection
B
Y strain
Colombian strain
IL-11Rα/GAPDH
1.50
1.25
1.00
0.75
0.50
0.25
0.00
CT
5
15
30
60
120
Days after infection
C
Y Heart
kDa
CT
5 d
30 d
60 d
120 d
CT
15 d
30 d
60 d
120 d
51
37
IL-11Rα
GAPDH
Colombian Heart
kDa
CT
5 d
15 d
30 d
60 d
CT
15 d
30 d
60 d
120 d
51
37
IL-11Rα
GAPDH
D
E
F
G
H
I
J
K
L
M

◂**Fig. 4** **A** Quantification of IL-11 in picograms per milligram in the hearts of uninfected control (CT) and infected mice with 1000 forms of the Y and Colombian strains at 5 ($n = 6$), 15 ($n = 6$), 30 ($n = 6$), 60 ($n = 6$), and 120 dpi ($n = 6$ for Y and $n = 11$ for Colombian). **B** IL-11Rα expression analyzed by Western Blotting in cardiac homogenates of control (CT) and infected mice with the Colombian or Y strains at 5 ($n = 6$), 15 ($n = 6$), 30 ($n = 6$), 60 ($n = 6$), and 120 dpi ($n = 6$). (B) IL-11Rα expression relative to GAPDH. **C** Representative bands of IL-11Rα expression in both strains at 5, 15, 30, 60, and 120 days of infection, with each band corresponding to an individual animal. Immunohistochemistry showing IL-11Rα labeling in mouse hearts: **D**, **E** and **F** Uninfected animals; **G**, **H**, and **I** Animals infected for 30, 60, and 120 days with the Colombian strain, respectively; **J**, **K**, **L** and **M** Animals infected for 15, 30, 60 and 120 days with the Y strain. *Statistically significant differences between infected and control (CT) groups, considering $p < 0.05$

Discussion

The genetic diversity of *Trypanosoma cruzi* (DTUs), along with host-related factors such as the initial immune response, are key determinants in the clinical outcome and pathogenesis of Chagas disease. However, there are still many gaps in our understanding of this process. This study explores important aspects of Chagas disease using *T. cruzi* strains from different DTUs in a murine model, evaluating the expression of IL-11 and its receptor IL-11Rα, as well as their potential relationship with the immune response and cardiac alterations across different stages of infection. the Colombian and Y strains belong to distinct DTU groups, TcI and TcII, respectively, which exhibit notable differences in virulence and pathogenicity in vertebrate hosts [34, 35]. Despite these differences, both strains are widely used in experimental models to investigate cardiac involvement in Chagas disease [30, 36, 37].

Infection with either TcI or TcII strains is known to induce a robust pro-inflammatory cytokine response, including IFN-γ, TNF-α, and IL-6, which are associated with host resistance to *T. cruzi* during the acute phase [6, 38–41]. However, the timing and intensity of this response varied depending on the infecting strain. In our study, the Y strain induced an early and intense pro-inflammatory response, with IFN-γ and IL-6 peaking at 15 days post-infection (dpi), TNF-α remaining elevated up to 30 dpi, and inflammatory infiltration persisting from 15 to 60 dpi. These intervals also coincided with high levels of parasitemia and tissue parasitism, both peaking at 15 dpi. In contrast, the Colombian strain elicited a more prolonged inflammatory response, starting at 15 dpi and sustained through 60 dpi, with elevated levels of pro-inflammatory cytokines during this period. In this case, parasitemia and tissue parasitism peaked at 30 dpi, and amastigote nests remained detectable in cardiac tissue until 120 dpi.

Heart weight, an important parameter for assessing acute myocarditis, typically associated with intense inflammatory infiltration, edema, and congestion [33], mirrored the inflammatory timeline observed for each strain, increasing at 15 dpi for the Y strain and at 30 dpi for the Colombian strain. These findings are consistent with the known characteristics of both strains, particularly the Colombian strain, which exhibits a sustained pro-inflammatory profile likely associated with its strong cardiac tropism [30, 33, 37, 42–44].

In contrast, and supporting the strain-specific immune dynamics observed, only the Y strain induced a regulatory cytokine profile at 30 dpi, with increased expression of IL-10 and IL-4. These cytokines help modulate the inflammatory response by suppressing IFN-γ, TNF-α, IL-12, and NO production [45–49]. The Colombian strain showed a sustained pro-inflammatory profile as evidenced by persistent amastigote nests and inflammatory mediators up to 120 dpi. Interestingly, IL-17, a cytokine commonly linked to pro-inflammatory responses [50, 51] was detected only in the Y strain at 30 dpi. Despite conflicting reports regarding its role in *T. cruzi* infection [52–54]. IL-17, along with IL-10 and IL-4, may contribute to immune modulation, helping to prevent excessive inflammation and limit cardiac damage during disease progression.

Taken together, these observations reinforce the idea that the distinct characteristics of each *T. cruzi* strain can shape disease progression and cardiac pathology through different immune responses. In light of this immunological landscape, our study also investigated the expression of IL-11, a cytokine increasingly associated with fibrosis but still poorly explored in the context of DC. In this sense, in the present study, *T. cruzi* infection did not induce significant IL-11 expression in the heart at any of the evaluated time points. As one of the first investigations to assess IL-11 production in Chagas disease, our finding, together with previous reports, suggest that IL-11 expression in this context is influenced by the genetic diversity of *T. cruzi* (DTUs).

Recently, Herreros-Cabello et al. [26] investigated IL-11 signaling through quantitative proteomic analysis of macrophages infected with different *T. cruzi* strains (Y and VFRA) and found that only the VFRA strain activated the IL-11 signaling pathway. However, the study did not present direct evidence of IL-11 expression, such as mRNA or protein levels. In a previous study, C2 C12 myoblasts were infected with strains from distinct DTUs: Brazil (TcI), Y (TcII), CL Brener and Tulahuen (TcVI), and only the Tulahuen strain induced IL-11 overexpression [27]. Based on these findings, it is noteworthy that both VFRA and Tulahuen strains belong to DTU VI, suggesting that IL-11 activation may be strain-dependent and influenced by the parasite's genetic background. This aligns with the results of our in vivo model, where neither the Colombian (TcI) nor Y (TcII) strains were able to induce cardiac IL-11 expression. Although in vitro models may not fully capture the immunological and tissue complexity

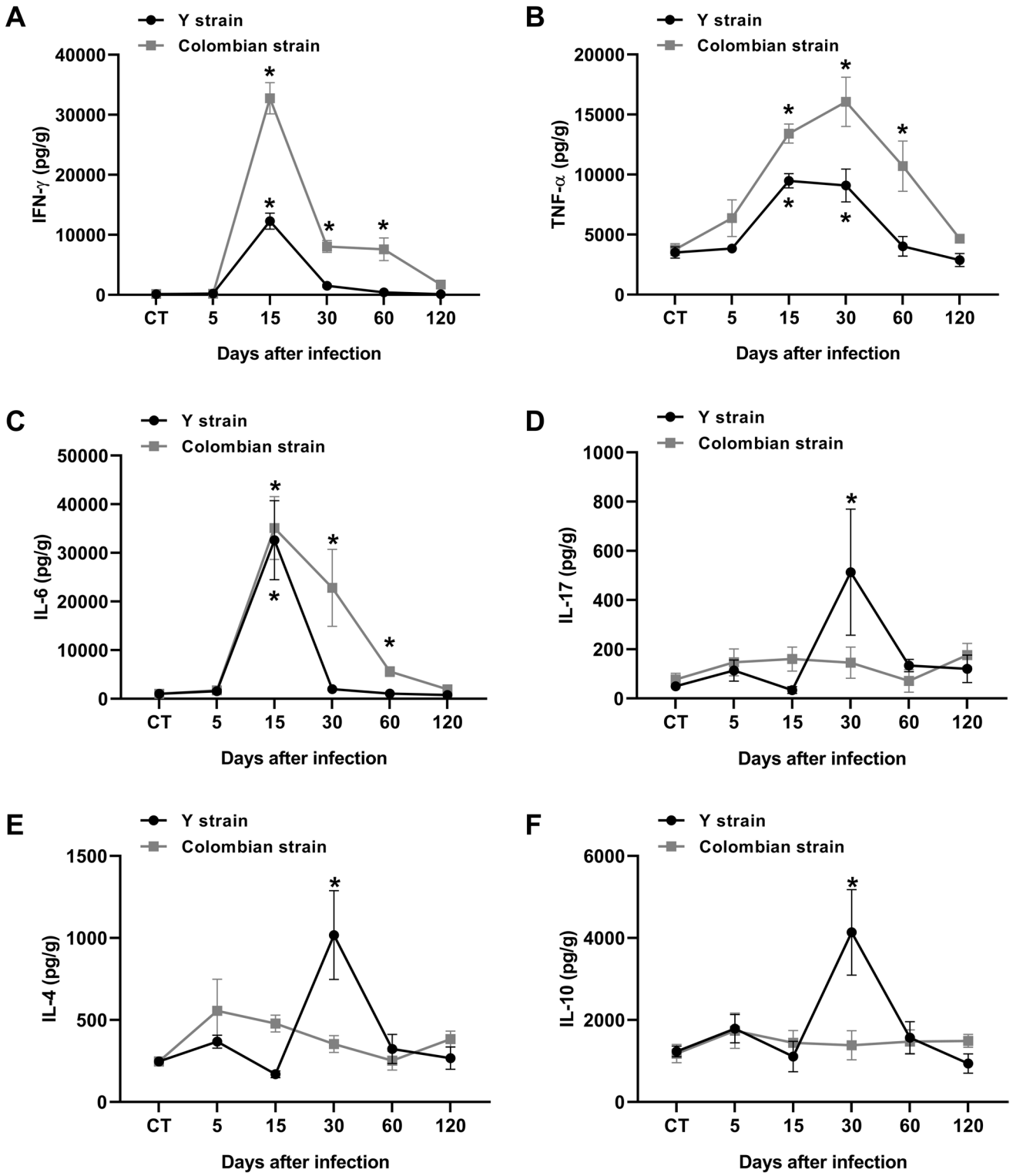

Fig. 5 Quantification of **A** IFN-γ, **B** TNF-α, **C** IL-6, **D** IL-17, **E** IL-4, and **F** IL-10 in picograms per gram in the hearts of uninfected control (CT) and infected mice with 1000 forms of the Y and Colombian strains at 5 ($n = 6$), 15 ($n = 6$), 30 ($n = 6$), 60 ($n = 6$), and 120 dpi ($n = 6$ for Y and $n = 11$ for Colombian). Quantification was conducted using the CBA method. *Statistically significant differences between infected and control (CT) groups, considering $p < 0.05$

of an infected host, all the data consistently indicate that IL-11 activation is specific and restricted to certain *T. cruzi* strains.

IL-11 is a member of the IL-6 cytokine family [55] and was initially described as an anti-inflammatory cytokine as it induces Th2 cell polarization and reduces cytokine expression, such as TNF-α, IL-1β, IL-6, IL-12 and NO in murine macrophages, while also promoting Th17 cell differentiation [18–21]. Recently, IL-11 has been described as a potent pro-inflammatory inducer in the heart of murine models, as it stimulates cardiomyocytes to produce IL-6, TNF, and chemokines such as Cxcl1, Cxcl5, Ccl4, and Ccl7 [56]. However, its dominant profile remains uncertain. In infectious diseases, IL-11's effects vary depending on the pathogen. In *E. coli*-induced pneumonia, for instance, IL-11 neutralization only reduced neutrophil accumulation [25]. In mice infected with *M. tuberculosis*, IL-11 inhibitors reduced IL-6, TNF-α, and IFN-γ production [23, 57–59]. While the dual role of IL-11 in infectious processes is evident, we believe that pathogen type and the microenvironment surrounding IL-11 are crucial in determining its influence on the immune system.

An interesting finding in our study is that, despite the non-significant expression of IL-11 in both strains, IL-11 receptor alpha (IL-11Rα) expression was clearly detected in cardiac tissue. Both strains induced IL-11Rα expression, which remained elevated up to 120 days post-infection. In the heart, cardiomyocytes, fibroblasts, macrophages, and endothelial cells can express IL-11Rα, which is normally expressed at low levels [20, 60]. The expression of this receptor has been associated with fibrosis in the kidney, liver, and lungs [22, 44, 45, 47, 61–64]. In different models of cardiac fibrosis, inhibition of IL-11 or IL-11Rα leads to reduced fibrosis, accompanied by downregulation of fibrosis-related genes such as *Col1a1, Col1a2, Col3a1, Fn1, Mmp2, Timp1,* and reduced activation of ERK signaling pathways [13, 14, 17, 65]. Similarly, in a murine model of acute pancreatitis, treatment with an anti-IL-11Rα antibody led to reductions in ERK, STAT, and NF-κB signaling, fibrosis, and pro-inflammatory cytokines, including TNF-α, IL-6, and IL-1β [66]. The involvement of IL-11/IL-11Rα-dependent ERK signaling is well established across multiple fibrotic conditions [17, 22, 67, 68].

During the progression of DC, the heart undergoes extensive tissue remodeling, characterized by fibroblast activation and increased collagen deposition. As a consequence of tissue injury caused by the inflammatory process triggered by *T. cruzi* infection, collagen accumulation becomes a hallmark of chronic Chagas cardiomyopathy [69, 70]. Cardiac fibrosis in Chagas disease has been strongly associated with ventricular dysfunction in humans [7] and has also been demonstrated in murine models [71, 72]. In our study, both *T. cruzi* strains induced significant collagen deposition: the Y strain from day 15 post-infection (dpi) and the Colombian strain from day 60 dpi. Notably, these time points coincided with the onset of IL-11Rα expression in cardiac tissue, and a positive correlation was observed between IL-11Rα levels and collagen accumulation. These findings are consistent with previous reports describing the pro-fibrotic role of IL-11Rα in various pathological settings and raise the hypothesis that this receptor may contribute similarly to fibrotic remodeling in Chagas cardiomyopathy.

The absence of significant IL-11 expression in our model raises important questions regarding the factors responsible for driving IL-11Rα expression in the heart. Although IL-11 levels were not statistically significant, the cytokine was still detectable in the cardiac tissue of infected animals. Even at basal levels, IL-11 may be sufficient to engage and activate its receptor. Additionally, IL-6, which shares the gp130 co-receptor with IL-11, activates similar downstream signaling pathways upon binding to its specific receptor, IL-6R [60]. It is therefore plausible that IL-6 could influence shared signaling cascades and indirectly modulate the expression of other cytokine receptors, including IL-11Rα. However, no direct evidence currently supports the notion that IL-6 or other cytokines regulate IL-11Rα expression.

In addition to cytokine signaling, cellular stress and tissue injury could be involved in the upregulation of IL-11Rα, independently of IL-11 itself. Thus, in cardiac, muscle or immune cells exposed to damage, IL-11Rα expression may function as a preparatory mechanism, making cells responsive if the ligand becomes available in higher concentrations at subsequent stages of infection. Furthermore, IL-11Rα is known to be highly expressed by cardiac fibroblasts [73], a cell type that plays a key role in fibrotic remodeling. The increased IL-11Rα expression observed in our model may therefore reflect not only cytokine-driven induction but also fibroblast expansion or activation within the cardiac microenvironment, which could sustain receptor expression up to 120 dpi. However, the mechanisms regulating this receptor remain incompletely understood. Nonetheless, further studies are needed to elucidate the regulatory mechanisms controlling IL-11Rα expression during *T. cruzi* infection and to clarify its functional role in Chagas-related cardiac fibrosis.

In summary, our findings demonstrate that IL-11 was detected in the heart during *T. cruzi* infection with both the Y (TcII) and Colombian (TcI) strains, although without statistically significant differences. In contrast, its receptor, IL-11Rα, showed sustained expression throughout the infection. The temporal correlation between IL-11Rα expression and collagen deposition suggests a potential role for this receptor in fibrotic remodeling on DC. These results support the notion that the genetic background of the parasite (DTUs) influences host immune and fibrotic responses, and that IL-11 and IL-11Rα may also contribute to this dynamic in a strain-dependent manner.

Nevertheless, some limitations of this study should be acknowledged. The analysis was restricted to 120 days post-infection; additional time points could help determine whether IL-11 expression emerges more prominently at later stages. Furthermore, only two *T. cruzi* strains (TcI and TcII) were evaluated. Including other DTUs—particularly TcVI, which has previously been associated with IL-11 activation—may provide broader insight into strain-specific effects. Notably, functional validation of IL-11Rα was not performed. Future studies employing functional approaches, such as IL-11Rα blockade or gene knockout models, are essential to elucidate the mechanistic role of this receptor in Chagas-related cardiac pathology and to assess its potential as a biomarker or therapeutic target in chronic Chagas cardiomyopathy.

Conclusions

Our findings demonstrate that the immune response and cardiac remodeling induced by different *Trypanosoma cruzi* DTUs are highly strain-dependent, with distinct impacts on inflammatory dynamics throughout the course of infection. IL-11 expression also appears to be strain-dependent; however, although IL-11 expression was not significantly induced in the strains analyzed (Colombiana TcI and Y TcII), the sustained upregulation of IL-11Rα and its correlation with collagen deposition suggest a potential role for this receptor in mediating cardiac fibrosis. These results reinforce the importance of parasite genetic diversity in the pathogenesis of Chagas disease and highlight the IL-11/IL-11Rα axis as a promising target for further investigation in the context of cardiac alterations during *T. cruzi* infection. Future studies should explore the regulatory mechanisms underlying IL-11Rα expression and its functional role in the progression of Chagas cardiomyopathy.

Supplementary Information The online version contains supplementary material available at https://doi.org/10.1007/s10753-025-02322-4.

Acknowledgements We express our gratitude to the Federal University of Triângulo Mineiro and the Federal University of Goiás for their support. This work was supported by Coordenação de Aperfeiçoamento de Pessoal de Nível Superior (CAPES – Grant number 001) and Conselho Nacional de Desenvolvimento Científico e Tecnológico (CNPQ).

Author contributions YLLB, JRdCN, PIRF, JFdO, ROT, FAdO, MRNC, MVdS, JRM were involved in the conception, design, and interpretation of the results. YLLB acquired the data. YLLB conducted the analyses and wrote the first draft of the manuscript. YLLB and JRM are the guarantors of this work; as such, they had full access to all the data in the study and take responsibility for the integrity of the data and the accuracy of the data analysis. All authors read and approved the final manuscript.

Funding This research received funding from Coordenação de Aperfeiçoamento de Pessoal de Nível Superior (CAPES–Grant number 001 and CAPES—Edital 009/2020), Conselho Nacional de Desenvolvimento Científico e Tecnológico (CNPQ–Bench fee 1b, 1 d and 2) and Fundação de Amparo à Pesquisa do Estado Minas Gerais (FAPEMIG—funding number: REDE313/16).

Data Availability Data is provided within the manuscript and supplementary information files.

Declarations

Ethics Approval The work was submitted and approved (ProtocolNo. 039/20; date: 03/22/2021) by the Comissão de Ética no Uso de Animais (CEUA) da Universidade Federal de Goiás (UFG), and all ethical aspects of animal handling were followed. In addition, the research group involved in the work was attentive to the behavior of the animals, on a daily basis, for the identification of humane endpoints if necessary.

Consent for Publication Not applicable.

Competing Interests The authors declare no competing interests.

References

1. Garg, Nisha J., Kevin M. Bonney, Stacey A. Kim, David M. Engman, and Daniel J. Luthringer. 2018. Pathology and Pathogenesis of Chagas Heart Disease. *Annual Review of Pathology: Mechanisms of Disease* 14:421–447. https://doi.org/10.1146/annurev-pathol-020117-043711.
2. Cunha-Neto, Edecio, and Christophe Chevillard. 2014. Chagas disease cardiomyopathy: Immunopathology and genetics. *Mediators of Inflammation* 2014. https://doi.org/10.1155/2014/683230.
3. Dias, João Carlos., Alberto Novaes Pinto, Eliane Dias Ramos, Alejandro Luquetti Gontijo, Maria Aparecida Shikanai-Yasuda, José Rodrigues. Coura, RosáliaMorais. Torres, et al. 2016. 2nd Brazilian Consensus on Chagas disease, 2015. *Revista da Sociedade Brasileira de Medicina Tropical* 49:3–60. https://doi.org/10.1590/0037-8682-0505-2016.
4. Rassi, Anis, Anis Rassi, and José Antonio Marin-Neto. 2009. Chagas heart disease: pathophysiologic mechanisms, prognostic factors and risk stratification. *Memórias do Instituto Oswaldo Cruz* 104. Instituto Oswaldo Cruz, Ministério da Saúde: 152–158. https://doi.org/10.1590/S0074-02762009000900021.
5. Henao-martínez, Andrés F, David A Schwartz, and Ivana V Yang. 2012. Chagasic cardiomyopathy, from acute to chronic: is this mediated by host. *Transactions of the Royal Society of Tropical Medicine and Hygiene* 106. Royal Society of Tropical Medicine

and Hygiene: 521–527. https://doi.org/10.1016/j.trstmh.2012.06.006.
6. Rodriguez, Hector O., Néstor A. Guerrero, Alen Fortes, Julien Santi-Rocca, Núria Gironès, and Manuel Fresno. 2014. Trypanosoma cruzi strains cause different myocarditis patterns in infected mice. *Acta Tropica* 139. Elsevier B.V.: 57–66. https://doi.org/10.1016/j.actatropica.2014.07.005.
7. Coura, José Rodrigues. 2007. Chagas disease: What is known and what is needed - A background article. *Memórias do Instituto Oswaldo Cruz* 102:113–122. https://doi.org/10.1590/s0074-02762007007500001.
8. Barretto, Antonio Carlos, Charles Mady Pereira, Edmundo Arteage-Fernandez, Noedir Stolf, Edgard Augusto Lopes, Maria de Lourdes, Giovanni Bellotti Higuchi, and Fulvio Pileggi. 1986. Right ventricular endomyocardial biopsy in chronic Chagas' disease. *American Heart Journal* 111:307–312. https://doi.org/10.1016/0002-8703(86)90144-4.
9. Rossi, Marcos A. 1998. *Fibrosis and inflammatory cells in human chronic chagasic myocarditis : Scanning electron microscopy and immunohistochemical observations* 66:183–194.
10. Adami, Eleonora, Sivakumar Viswanathan, Anissa A. Widjaja, Benjamin Ng, Sonia Chothani, Nevin Zhihao, Jessie Tan, et al. 2021. IL11 is elevated in systemic sclerosis and IL11-dependent ERK signalling underlies TGFβ-mediated activation of dermal fibroblasts. *Rheumatology (United Kingdom)* 60:5820–5826. https://doi.org/10.1093/rheumatology/keab168.
11. Lim, Wei Wen, Ben Corden, Benjamin Ng, Konstantinos Vanezis, Giuseppe D'Agostino, Anissa A. Widjaja, Wei Hua Song, et al. 2020. Interleukin-11 is important for vascular smooth muscle phenotypic switching and aortic inflammation, fibrosis and remodeling in mouse models. *Scientific Reports* 10. Nature Publishing Group UK: 1–18. https://doi.org/10.1038/s41598-020-74944-7.
12. Ng, Benjamin, Jinrui Dong, Giuseppe D'Agostino, Sivakumar Viswanathan, Anissa A. Widjaja, Wei Wen Lim, Nicole S.J.. Ko, et al. 2019. Interleukin-11 is a therapeutic target in idiopathic pulmonary fibrosis. *Science Translational Medicine* 11:1–15. https://doi.org/10.1126/scitranslmed.aaw1237.
13. Schafer, Sebastian, Sivakumar Viswanathan, Anissa A. Widjaja, Wei Wen Lim, Aida Moreno-Moral, Daniel M. DeLaughter, Benjamin Ng, et al. 2017. IL-11 is a crucial determinant of cardiovascular fibrosis. *Nature* 552. Nature: 110–115. https://doi.org/10.1038/NATURE24676.
14. Braga, Yarlla Loyane Lira, José Rodrigues do Carmo Neto, Pablo Igor Ribeiro Franco, Fernanda Rodrigues Helmo, Marlene Antônia dos Reis, Flávia Aparecida de Oliveira, Mara Rúbia Nunes Celes, Marcos Vinícius da Silva, and Juliana Reis Machado. 2024. The Influence of IL-11 on Cardiac Fibrosis in Experimental Models: A Systematic Review. *Journal of Cardiovascular Development and Disease* 11. Multidisciplinary Digital Publishing Institute (MDPI): 65. https://doi.org/10.3390/JCDD11020065.
15. Bai, Xin, Guolin Zhao, Qijing Chen, Zhongyu Li, Mingzhu Gao, William Ho, Xu. Xiaoyang, and Xue Qing Zhang. 2022. Inhaled siRNA nanoparticles targeting IL11 inhibit lung fibrosis and improve pulmonary function post-bleomycin challenge. *Science Advances* 8:1–18. https://doi.org/10.1126/sciadv.abn7162.
16. Corden, Ben, Wei Wen Lim, Weihua Song, Xie Chen, Nicole S.J.. Ko, Su. Liping, Nicole G.Z.. Tee, Eleonora Adami, Sebastian Schafer, and Stuart A. Cook. 2021. Therapeutic Targeting of Interleukin-11 Signalling Reduces Pressure Overload-Induced Cardiac Fibrosis in Mice. *Journal of Cardiovascular Translational Research* 14:222–228. https://doi.org/10.1007/s12265-020-10054-z.
17. Lim, Wei Wen, Ben Corden, Lei Ye, Sivakumar Viswanathan, Anissa A. Widjaja, Chen Xie, Liping Su, Nicole G.Z. Tee, Sebastian Schafer, and Stuart A. Cook. 2021. Antibody-mediated neutralization of IL11 signalling reduces ERK activation and cardiac fibrosis in a mouse model of severe pressure overload. *Clinical and experimental pharmacology & physiology* 48. Clin Exp Pharmacol Physiol: 605–613. https://doi.org/10.1111/1440-1681.13458.
18. Liebert, Mary Ann, Mary Bozza, Judith L Bliss, Andrew J Dorner, and William L Trepicchio. 2001. Interleukin-11 Modulates Th1 / Th2 Cytokine Production 30: 21–30.
19. Curti, Antonio, Marina Ratta, Silvia Corinti, Giampiero Girolomoni, Francesca Ricci, Pierluigi Tazzari, Michela Siena, et al. 2001. Interleukin-11 induces Th2 polarization of human CD4+ T cells. *Blood* 97:2758–2763. https://doi.org/10.1182/blood.V97.9.2758.
20. Xu, Dixon H., Ziwen Zhu, Mark R. Wakefield, Huaping Xiao, Qian Bai, and Yujiang Fang. 2016. *The role of IL-11 in immunity and cancer*. *Cancer Letters*. Vol. 373. Elsevier Ireland Ltd. https://doi.org/10.1016/j.canlet.2016.01.004.
21. Zhang, Xin, Nazanin Kiapour, Sahil Kapoor, Joseph R. Merrill, Yongjuan Xia, Woomi Ban, Stephanie M. Cohen, et al. 2018. IL-11 antagonist suppresses Th17 cell-mediated neuroinflammation and demyelination in a mouse model of relapsing-remitting multiple sclerosis. *Clinical Immunology* 197. Elsevier Inc: 45–53. https://doi.org/10.1016/j.clim.2018.08.006.
22. Chen, Haiyun, Hongjie Chen, Jialong Liang, Xin Gu, Jiawen Zhou, Chunfeng Xie, Xianhui Lv, et al. 2020. TGF-β1/IL-11/MEK/ERK signaling mediates senescence-associated pulmonary fibrosis in a stress-induced premature senescence model of Bmi-1 deficiency. *Experimental and Molecular Medicine* 52. Springer US: 130–151. https://doi.org/10.1038/s12276-019-0371-7.
23. Kapina, Marina A., Galina S. Shepelkova, Vadim G. Avdeenko, Anna N. Guseva, Tatiana K. Kondratieva, Vladimir V. Evstifeev, and Alexander S. Apt. 2011. Interleukin-11 drives early lung inflammation during mycobacterium tuberculosis infection in genetically susceptible mice. *PLoS ONE* 6. https://doi.org/10.1371/journal.pone.0021878.
24. Lawitz, Eric J., Matthew J. Hepburn, and Thomas J. Casey. 2004. A pilot study of interleukin-11 in subjects with chronic hepatitis C and advanced liver disease nonresponsive to antiviral therapy. *American Journal of Gastroenterology* 99:2359–2364. https://doi.org/10.1111/j.1572-0241.2004.40047.x.
25. Traber, Katrina E., Ernest L. Dimbo, Elise M. Symer, Filiz T. Korkmaz, Matthew R. Jones, Joseph P. Mizgerd, and Lee J. Quinton. 2019. Roles of interleukin-11 during acute bacterial pneumonia. *PLoS ONE* 14:1–16. https://doi.org/10.1371/journal.pone.0221029.
26. Herreros-Cabello, Alfonso, Javier del Moral-Salmoral, Esperanza Morato, Anabel Marina, Beatriz Barrocal, Manuel Fresno, and Núria Gironès. 2024. Quantitative Proteomic Analysis of Macrophages Infected with Trypanosoma cruzi Reveals Different Responses Dependent on the SLAMF1 Receptor and the Parasite Strain. *International Journal of Molecular Sciences* 25. Multidisciplinary Digital Publishing Institute (MDPI): 7493. https://doi.org/10.3390/IJMS25137493/S1.
27. Nisimura, Lindice M., Laura L. Coelho, Tatiana G. de Melo, Paloma de Carvalho Vieira, Pedro H. Victorino, Luciana R. Garzoni, David C. Spray, et al. 2020. Trypanosoma cruzi Promotes Transcriptomic Remodeling of the JAK/STAT Signaling and Cell Cycle Pathways in Myoblasts. *Frontiers in Cellular and Infection Microbiology* 10. Frontiers Media S.A.: 255. https://doi.org/10.3389/FCIMB.2020.00255/FULL.
28. Błyszczuk, Przemysław. 2019. Myocarditis in Humans and in Experimental Animal Models. *Frontiers in Cardiovascular Medicine* 6:1–17. https://doi.org/10.3389/fcvm.2019.00064.
29. Borges, Cláudia Renata., Marlene Antônia Bibiano, Lúcio. dos Reis, Roberto Castellano, Edjane Souza Santos, Virmondes Rodrigues Junior, Denise Bertulucci Rocha. Rodrigues, Javier

Emilio Lazo. Chica, Sanívia Aparecida, and de Lima Pereira. 2009. Papel do óxido nítrico no desenvolvimento de lesões cardíacas na fase aguda da infecção experimental pelo Trypanosoma cruzi. *Revista da Sociedade Brasileira de Medicina Tropical* 42:170–174. https://doi.org/10.1590/s0037-86822009000200015.

30. Wesley, Moisés, Aline Moraes, Ana de Cássia Rosa, Juliana Lott Carvalho, Tatiana Shiroma, Tamires Vital, Nayra Dias, et al. 2019. Correlation of parasite burden, kdna integration, autoreactive antibodies, and cytokine pattern in the pathophysiology of chagas disease. *Frontiers in Microbiology* 10. https://doi.org/10.3389/fmicb.2019.01856.
31. Sanches, Tiago L.M.., Larissa D. Cunha, Grace K. Silva, Paulo M.M.. Guedes, João Santana. Silva, and Dario S. Zamboni. 2014. The use of a heterogeneously controlled mouse population reveals a significant correlation of acute phase parasitemia with mortality in Chagas disease. *PLoS ONE* 9:1–8. https://doi.org/10.1371/journal.pone.0091640.
32. Brener, Z. 1962. Therapeutic activity and criterion of cure on mice experimentally infected with Trypanosoma cruzi. *Revista do Instituto de Medicina Tropical de São Paulo* 4:389–396.
33. Braga, Yarlla L.L., José R.C. Neto, Arthur W.F. Costa, Muriel V.T. Silva, Marcos V. Silva, Mara R.N. Celes, Milton A.P. Oliveira, et al. 2022. Interleukin-32 γ in the Control of Acute Experimental Chagas Disease. *Journal of Immunology Research* 2022. https://doi.org/10.1155/2022/7070301.
34. Zingales, B. 2009. S G Andrade, D A Campbell, E Chiari, O Fernandes, and F Guhl. *A new consensus for Trypanosoma cruzi intraspecific nomenclature : Second revision meeting recommends TcI to TcVI* 104:1051–1054.
35. Nisimura, Lindice M., Laura L. Coelho, Tatiana G. de Melo, Paloma de Carvalho, Pedro H. Vieira, Luciana R. Victorino, David C. Garzoni, Spray, et al. 2020. Trypanosoma cruzi Promotes Transcriptomic Remodeling of the JAK/STAT Signaling and Cell Cycle Pathways in Myoblasts. *Frontiers in Cellular and Infection Microbiology* 10:1–15. https://doi.org/10.3389/fcimb.2020.00255.
36. Mata-Santos, Hilton Antônio, Camila Victória Sousa. Oliveira, Daniel F. Feijo, Daniel Figueiredo Vanzan, Glaucia Vilar-Pereira, Isalira P. Ramos, VitorCoutinho Carneiro, et al. 2024. Heart function enhancement by an Nrf2-activating antioxidant in acute Y-strain Chagas disease, but not in chronic Colombian or Y-strain. *PLOS Neglected Tropical Diseases* 18 : e0012612. https://doi.org/10.1371/JOURNAL.PNTD.0012612.
37. Reis Machado, Juliana, Marcos Vinícius Silva, Diego Costa Borges, Crislaine Aparecida Da Silva, Luis Eduardo Ramirez, Marlene Antônia Dos Reis, Lúcio Roberto Castellano, Virmondes Rodrigues, and Denise Bertulucci Rocha Rodrigues. 2014. Immunopathological aspects of experimental trypanosoma cruzi reinfections. *BioMed Research International* 2014. https://doi.org/10.1155/2014/648715.
38. Cardillo, Fabíola, Julio C. Voltarelli, Steven G. Reed, and João. S. Silva. 1996. Regulation of Trypanosoma cruzi infection in mice by gamma interferon and interleukin 10: Role of NK cells. *Infection and Immunity* 64:128–134.
39. de Araújo, Fernanda, Danielle Marquete Fortes, Andréa Teixeira-Carvalho. Vitelli-Avelar, Paulo Renato Zuquim. Antas, Juliana Assis Silva. Gomes, Renato Sathler-Avelar, ManoelOtávio Costa. Rocha, et al. 2011. Regulatory T cells phenotype in different clinical forms of chagas' disease. *PLoS Neglected Tropical Diseases* 5:1–8. https://doi.org/10.1371/journal.pntd.0000992.
40. Silva, Joao S., Daniel R. Twardzik, and Steven G. Reed. 1991. Regulation of Trypanosoma cruzi infections in vitro and in vivo by transforming growth factor beta (TGF-beta). *The Journal of experimental medicine* 174:539–545. https://doi.org/10.1084/jem.174.3.539.
41. Silva, Joao S. 1994. Interleukin 10 and interferon gamma regulation of experimental Trypanosoma cruzi infection. *Journal of Experimental Medicine* 175:169–174. https://doi.org/10.1084/jem.175.1.169.
42. Queiroga, TamyresBernadete Dantas, NathalieSena de Pereira, DenisDantas da Silva, CléberMesquita. de Andrade, RaimundoFernandesAraújo. de Júnior, CarlosRamonNascimento. do Brito, LúciaMariaCunha. da Galvão, AntôniaCláudiaJácome. da Câmara, ManuelaSalesLima. Nascimento, and PauloMarcos-Matta. Guedes. 2021. Virulence of Trypanosoma cruzi Strains Is Related to the Differential Expression of Innate Immune Receptors in the Heart. *Frontiers in Cellular and Infection Microbiology* 11:1–14. https://doi.org/10.3389/fcimb.2021.696719.
43. Andrade, Sonia Gumes, Maria Luiza Carvalho, and Rozália M. Figueira. 1970. *Caracterização morfo-biológica e histopatologica de diferentes cêpas do Trypanosoma cruzi*. Bahia: Gaz. méd.
44. Michailowsky, Vladimir, Neide M. Silva, Carolina D. Rocha, Leda Q. Vieira, Joseli Lannes-Vieira, and Ricardo T. Gazzinelli. 2001. Pivotal role of interleukin-12 and interferon-γ axis in controlling tissue parasitism and inflammation in the heart and central nervous system during Trypanosoma cruzi infection. *American Journal of Pathology* 159:1723–1733. https://doi.org/10.1016/S0002-9440(10)63019-2.
45. Abrahamsohn, Ises A., and Robert L. Coffman. 1996. Trypanosoma cruzi: IL-10, TNF, IFN-gamma, and IL-12 regulate innate and acquired immunity to infection. *Experimental Parasitology* 84:231–244. https://doi.org/10.1006/EXPR.1996.0109.
46. Cardillo, Fabíola, Rosa Teixeira, Paulo de Pinho, Renato Zuquim Antas, and José Mengel. 2015. Immunity and immune modulation in Trypanosoma cruzi infection. *Pathogens and disease* 73:082. https://doi.org/10.1093/femspd/ftv082.
47. da Silva, Marcos Vinicius, AlineCristinaSouza. da Silva, MaraRúbiaNunes. Celes, JulianaReis Machado, MariaLuízaGonçalves-Reis. dos Monteiro, RuySousa de Lino-Júnior, NatáliaCarasek-Matos. Cascudo, et al. 2018. Upregulation of Cardiac IL-10 and Downregulation of IFN- γ in Balb/c IL-4 −/− in Acute Chagasic Myocarditis due to Colombian Strain of Trypanosoma cruzi. *Mediators of Inflammation* 2018:1–9. https://doi.org/10.1155/2018/3421897.
48. Hiyama, Kazutoshi, Shinjiro Hamano, Takahiko Nakamura, Kikuo Nomoto, and Isao Tada. 2001. IL-4 reduces resistance of mice to Trypanosoma cruzi infection. *Parasitology Research* 87:269–274. https://doi.org/10.1007/PL00008577.
49. Soares, M. B. P., K. N. Silva-Mota, R. S. Lima, M. C. Bellintani, L. Pontes-de-Carvalho, and R. Ribeiro-dos-Santos. 2001. Modulation of chagasic cardiomyopathy by interleukin-4: Dissociation between inflammation and tissue parasitism. *American Journal of Pathology* 159:703–709. https://doi.org/10.1016/S0002-9440(10)61741-5.
50. Miyazaki, Y., S. Hamano, S. Wang, Y. Shimanoe, Y. Iwakura, and H. Yoshida. 2010. IL-17 Is Necessary for Host Protection against Acute-Phase Trypanosoma cruzi Infection. *The Journal of Immunology* 185:1150–1157. https://doi.org/10.4049/jimmunol.0900047.
51. Boari, Jimena Tosello, Cintia L. Araujo Furlan, Facundo Fiocca Vernengo, Constanza Rodriguez, María C. Ramello, María C. Amezcua Vesely, Melisa Gorosito Serrán, et al. 2018. IL-17RA-signaling modulates CD8+ T Cell survival and exhaustion during trypanosoma cruzi infection. *Frontiers in Immunology* 9. Frontiers Media S.A.: 2347. https://doi.org/10.3389/FIMMU.2018.02347/FULL
52. Guedes, Paulo Marcos, Renata Dellalibera-Joviliano. Matta, André Schmidt, Fredy Roberto Salazar. Gutierrez, João Santana. Silva, Anis Rassi, Gerson Jhonatan Rodrigues, et al. 2012.

Deficient Regulatory T Cell Activity and Low Frequency of IL-17-Producing T Cells Correlate with the Extent of Cardiomyopathy in Human Chagas' Disease. *PLoS Neglected Tropical Diseases* 6:e1630. https://doi.org/10.1371/journal.pntd.0001630.

53. Magalhães, M. D. Luisa, N. A. FernandaVillani, MariaCarmoP. do Nunes, JKenneth Gollob, OCManoel. Rocha, OWalderez Dutra, J. Kenneth, Gollob, and FernandaNA. Villani. 2012. High Interleukin 17 Expression Is Correlated With Better Cardiac Function in Human Chagas Disease. *The Journal of Infectious Diseases* 207:661–665. https://doi.org/10.1093/infdis/jis724.
54. Sousa, Giovane R., Juliana A.S. Gomes, Marcos Paulo S. Damasio, Maria Carmo P. Nunes, Henrique S. Costa, Nayara I. Medeiros, Rafaelle C.G. Fares, Ana Thereza Chaves, Rodrigo Corrêa-Oliveira, and Manoel Otávio C. Rocha. 2017. The role of interleukin 17-mediated immune response in Chagas disease: High level is correlated with better left ventricular function. *PLoS ONE* 12. Public Library of Science: e0172833. https://doi.org/10.1371/JOURNAL.PONE.0172833.
55. Du, Xunxiang, and David A. Williams. 1997. Interleukin-11: Review of Molecular, Cell Biology, and Clinical Use. *The Journal of The American Society of Hematology* 89
56. Sweeney, Mark, Katie O'Fee, Chelsie Villanueva-Hayes, Ekhlas Rahman, Michael Lee, Konstantinos Vanezis, Ivan Andrew, et al. 2023. Cardiomyocyte-Restricted Expression of IL11 Causes Cardiac Fibrosis, Inflammation, and Dysfunction. *International Journal of Molecular Sciences* 24. https://doi.org/10.3390/ijms241612989.
57. Kondratieva, Tatiana, Margarita Shleeva, Marina Kapina, Elvira Rubakova, Irina Linge, Alexander Dyatlov, Elena Kondratieva, Arseny Kaprelyants, and Alexander Apt. 2020. Prolonged infection triggered by dormant Mycobacterium tuberculosis: Immune and inflammatory responses in lungs of genetically susceptible and resistant mice. *PLoS ONE* 15:1–11. https://doi.org/10.1371/journal.pone.0239668.
58. Ritter, Kristina, Jasmin Rousseau, and Christoph Hölscher. 2020. The Role of gp130 Cytokines in Tuberculosis. *Cells* 9:1–28. https://doi.org/10.3390/cells9122695.
59. Shepelkova, Galina, Vladimir Evstifeev, Konstantin Majorov, Irina Bocharova, and Alexander Apt. 2016. Therapeutic Effect of Recombinant Mutated Interleukin 11 in the Mouse Model of Tuberculosis. *Journal of Infectious Diseases* 214:496–501. https://doi.org/10.1093/infdis/jiw176.
60. Garbers, Christoph, and Jürgen. Scheller. 2013. Interleukin-6 and interleukin-11: same same but different. *Biological Chemistry* 394:1145–1161. https://doi.org/10.1515/hsz-2013-0166.
61. Corden, Benjamin, Eleonora Adami, Mark Sweeney, Sebastian Schafer, and Stuart A. Cook. 2020. IL-11 in cardiac and renal fibrosis: Late to the party but a central player. *British Journal of Pharmacology* 177:1695–1708. https://doi.org/10.1111/bph.15013.
62. Ng, Benjamin, Jinrui Dong, Sivakumar Viswanathan, Anissa A. Widjaja, Bhairav S. Paleja, Eleonora Adami, Nicole S.J.. Ko, et al. 2020. Fibroblast-specific IL11 signaling drives chronic inflammation in murine fibrotic lung disease. *FASEB Journal* 34:11802–11815. https://doi.org/10.1096/fj.202001045RR.
63. Dong, Jinrui, Sivakumar Viswanathan, Eleonora Adami, Brijesh K. Singh, Sonia P. Chothani, Benjamin Ng, Wei Wen Lim, et al. 2021. Hepatocyte-specific IL11 cis-signaling drives lipotoxicity and underlies the transition from NAFLD to NASH. *Nature Communications* 12:1–15. https://doi.org/10.1038/s41467-020-20303-z.
64. Milara, Javier, Inés. Roger, Paula Montero, Enrique Artigues, Juan Escrivá, Raquel Del Río, and Julio Cortijo. 2024. Targeting IL-11 to reduce fibrocyte circulation and lung accumulation in animal models of pulmonary hypertension-associated lung fibrosis. *British Journal of Pharmacology* 181:2991–3009. https://doi.org/10.1111/bph.16393.
65. Chen, Youming, Lan Wang, Shixing Huang, Jiangfeng Ke, Qing Wang, Zhiwen Zhou, and Wei Chang. 2021. Lutein attenuates angiotensin II- induced cardiac remodeling by inhibiting AP-1/IL-11 signaling. *Redox biology* 44:102020. https://doi.org/10.1016/J.REDOX.2021.102020.
66. Ng, Benjamin, Sivakumar Viswanathan, Anissa A. Widjaja, Wei Wen Lim, Shamini G. Shekeran, Joyce Wei Ting Goh, Jessie Tan, et al. 2022. IL11 Activates Pancreatic Stellate Cells and Causes Pancreatic Inflammation, Fibrosis and Atrophy in a Mouse Model of Pancreatitis. *International Journal of Molecular Sciences* 23. https://doi.org/10.3390/ijms23073549.
67. Widjaja, Anissa, Brijesh Singh, Eleonora Adami, Sivakumar Viswanathan, Giuseppe D'Agostino, Jinrui Dong, Benjamin Ng, et al. 2018. IL-11 neutralising therapies target hepatic stellate cell-induced liver inflammation and fibrosis in NASH. *bioRxiv*: 470062. https://doi.org/10.1101/470062.
68. Wu, Fan, Yan Zhao, Qingqing Shao, Ke. Fang, Ruolan Dong, Shujun Jiang, Lu. Fuer, Jinlong Luo, and Guang Chen. 2021. Ameliorative Effects of Osthole on Experimental Renal Fibrosis in vivo and in vitro by Inhibiting IL-11/ERK1/2 Signaling. *Frontiers in Pharmacology* 12:1–13. https://doi.org/10.3389/fphar.2021.646331.
69. Marin-Neto, Jose Antonio, Edécio. Cunha-Neto, Benedito C. Maciel, and Marcus V. Simões. 2007. Pathogenesis of chronic Chagas heart disease. *Circulation* 115:1109–1123. https://doi.org/10.1161/CIRCULATIONAHA.106.624296.
70. Simões, Marcus Vinicius, KárytaSuelyMacedo. Martins, André Schmidt, Minna Moreira Dias. Romano, and José Antonio. Marin-Neto. 2018. Chagas Disease Cardiomyopathy. *International Journal of Cardiovascular Sciences* 31:173–189. https://doi.org/10.5935/2359-4802.20180011.
71. Bertelli, Adriano, Liliana M Sanmarco, Carla A Pascuale, Miriam Postan, and Martin Craig Taylor. 2020. Anti-inflammatory Role of Galectin-8 During Trypanosoma cruzi Chronic Infection 10:1–12. https://doi.org/10.3389/fcimb.2020.00285.
72. Novaes, Rômulo D., Arlete R. Penitente, Reggiani V. Gonçalves, André Talvani, Maria C G Peluzio, Clóvis A. Neves, Antônio J. Natali, and Izabel R S C Maldonado. 2013. Trypanosoma cruzi infection induces morphological reorganization of the myocardium parenchyma and stroma, and modifies the mechanical properties of atrial and ventricular cardiomyocytes in rats. *Cardiovascular Pathology* 22. Elsevier Inc.: 270–279. https://doi.org/10.1016/j.carpath.2012.12.001.
73. Widjaja, Anissa A., Sivakumar Viswanathan, Dong Jinrui, Brijesh K. Singh, Jessie Tan, Joyce Goh Wei. Ting, David Lamb, et al. 2021. Molecular Dissection of Pro-Fibrotic IL11 Signaling in Cardiac and Pulmonary Fibroblasts. *Frontiers in Molecular Biosciences* 8:1–14. https://doi.org/10.3389/fmolb.2021.740650.